Omics profiling identifies MAPK/ERK pathway as a gatekeeper of nephron progenitor metabolism

Hyuk Nam Kwon[1,2], Kristen Kurtzeborn[1,2], Xing Jin[3], Bruno Reversade[4], Sunghyouk Park[3], and Satu Kuure[1,2,5#]

[1]Helsinki Institute of Life Science, University of Helsinki, Finland

[2]Stem Cells and Metabolism Research Program, Faculty of Medicine, University of Helsinki, Finland

[3]Collge of Pharmacy, Natural Product Research Institute, Seoul National University, Seoul, Korea

[4]Institute of Medical Biology, A*STAR, Singapore 138648, Singapore

[5]Stem Cells and Metabolism Research Program, Faculty of Medicine, University of Helsinki, Helsinki, Finland

[5]GM-unit, Laboratory Animal Center, Helsinki Institute of Life Science, University of Helsinki, Finland

[#]Correspondence: satu.kuure@helsinki.fi

Keywords: organogenesis, tissue-specific progenitors, self-renewal, differentiation, development, metabolism, receptor tyrosine kinase signaling, intracellular signaling cascades

ABSTRACT

Nephron endowment is defined by fetal kidney growth and it critically dictates renal health in adults. Despite the advances in understanding the molecular regulation of nephron progenitor maintenance, propagation, and differentiation, the causes for low congenital nephron count and contribution of basic metabolism to nephron progenitor regulation remain poorly studied. Here we have analyzed the metabolic effects that depend on and are triggered by the mitogen-activated protein kinase/extracellular signal-regulated kinase (MAPK/ERK) pathway, which is an essential intracellular cascade required for nephron progenitor maintenance. Our combined approach utilizing LC/MS-based metabolomics and transcriptional profiling of MAPK/ERK-deficient cells identified 18 out of total 46 metabolites (38 untargeted and 8 targeted) that were down-regulated. These represent glycolysis, gluconeogenesis, pentose phosphate, glycine, and proline pathways among others. We focused our functional characterization of identified metabolites on pyruvate and proline. Use of *in vitro* kidney cultures revealed dosage-specific functions for pyruvate in not only controlling ureteric bud branching but also determining progenitor and differentiated (tip-trunk) cell identities. Our *in vivo* characterization of *Pycr1/2* double knockout kidneys revealed functional requirement for proline metabolism in nephron progenitor maintenance. In summary, our results demonstrate that MAPK/ERK cascade regulates energy and amino acid metabolism in developing kidney where these metabolic pathways specifically regulate progenitor preservation.

INTRODUCTION

The differentiation capacity of embryonic nephron progenitors (NP) is crucial factor for renal health later in life as the extend of fetal nephrogenesis determines individual's final nephron number, and low nephron count predicts a higher risk for renal complications (1, 2). Embryonic kidney development is orchestrated by intercellular and intracellular signaling taking place between the two mesodermal derivatives, the ureteric bud (UB) and metanephric mesenchyme (MM) (3, 4). The UB branching patterns and expands kidney in size while MM hosts NPs, which give rise to all segments of functional nephron (5). UB together with the MM form NP niche where balanced propagation and differentiation of MM-residing progenitors are guided by niche intrinsic and extrinsic cues (6).

The total NP lifespan is limited to fetal period in humans and to the first postnatal days of life in mouse (7-9). The molecular regulation of NP maintenance and differentiation has been extensively studied (10, 11), but the factors contributing to the cessation of nephrogenic program are only evolving and suggest involvement of changes in signal transduction activities (12-14). Moreover, very little is known about metabolic events and especially mitochondrial metabolism underlying the specific behaviors of NPs during their propagation and differentiation switches. A recent study demonstrated higher glycolysis dependance in younger than older NPs and showed that glycolysis inhibition promotes differentiation (15). Von Hippel-Lindau (VHL) tumor suppressor appears important for mitochondrial respiration in NPs, which show mild differentiation deficiency in the NP-specific absence of *Vhl* (16).

Although one of the major mitochondrial metabolites, namely pyruvate, is essential for normal early embryonic development (17, 18), detailed understanding of its functions in organogenesis is missing. Production of pyruvate is regulated by the embryonic kidney expressed glycolytic enzyme pyruvate kinase isozyme M2 (PKM2), which function is controlled by the mitogen-activated protein kinase/extracellular signal-regulated kinase (MAPK/ERK) (19). We have

recently demonstrated the importance of MAPK/ERK activity in mediating extracellular signals to NP regulation, where it on one hand maintains NP identity and on the other hand propels differentiation in nephron precursors (11, 20, 21). Interestingly, MAPK/ERK target p53 is shown to ensure metabolic fitness in propagating nephron progenitors (22). The p53 target Rrm2b, encoding a catalytic subunit of ribonucleotide reductase (p53R2), is required for nephron function and interestingly interacts with mitochondrial proline synthesis enzymes pyrroline-5-carboxylate reductase (PYCR) 1 and 2 (23-25). Proline metabolism is heavily utilized in cancer cells and its synthesis deficiencies are recently identified causative for many congenital disorders (26, 27). Single and double knockout studies of *Pycr1* and -2 support the essential involvement of proline metabolisms in neuronal differentiation (28, 29), but its organ and tissue-specific requirements remain elusive.

We have utilized a systems biology approach to study the cellular functions that MAPK/ERK activity effectuates in NPs. Our combined RNA sequencing and metabolomics characterization of control and MAPK/ERK-deficient NPs revealed cellular metabolism as one of the most important contributing factors in their regulation. These results establish that MAPK/ERK pathway guides nephrogenesis in developing kidney through regulating energy metabolism in NPs.

RESULTS

Gene Ontology Analysis and Pathway Analysis

Recently, our group utilized genetic approach to reveal critical roles for nephron progenitor-specific MAPK/ERK signaling in their maintenance and propagation (20). Total of over 5,000 differentially expressed genes (DEGs) were identified in the genetic model of MAPK/ERK-deficient nephron progenitor (NP) populations among which significant effects on mitochondrial energy metabolism were revealed (Kurtzeborn et al, manuscript in revision). To investigate more in depth mitochondrial metabolism in NP populations, we now performed the

biological interpretation analysis of the RNAseq data from NPs using Cytoscape plug-in ClueGO (30, 31).

ClueGO enables functional interpretation of huge gene lists and creates gene ontology (GO)/pathway term network which reflects the parallel relationship based on the similarity of associated genes. Figure 1A shows an overview of the GO analysis of DEGs from NP population with criterion of Padj<0.05 and fold change of │log2fold change│≥2. Additionally, GO analysis to down-regulated (Figure 1B) and up-regulated DEGs (Figure 1C) were also operated by integrating one of the GO Consortium class "cellular component" as well as Kyoto Encyclopedia of Genes and Genomes (KEGG) database pathway (32, 33). As shown in Figure 1A, oxidative phosphorylation (18.87%) and mitochondrion (11.32%), which represent mitochondrial metabolism, account for a total of 30.19% of cellular functions affected by MAPK/ERK pathway. This means that the mitochondrial metabolism represents the largest portion of (nearly one-third) cellular pathways that depend on MAPK/ERK. According to characterization of down-regulated DEG results (Figure 1B), mitochondrial inner membrane (25.0%) and mitochondrion (15.0%) account for 40.0% of the down-regulated gene expressions strongly suggesting down-regulated mitochondrial metabolism in the absence of MAPK/ERK activation. The up-regulated genes were so scattered and few that their pathway analysis failed to provide meaningful outcome, although many of them associate with oxidative phosphorylation (Table S1). This likely reflects compensatory effect, which tries to increase oxidative phosphorylation process in a situation of reduced mitochondrial inner membrane gene expressions. The list of genes that make up the GO term on Figure 1 is summarized in supplementary Table S1.

Metabolomics analysis of MAPK/ERK-deficiency

As GO analysis showed significantly affected mitochondrial metabolism in MAPK/ERK-deficient NPs, we next applied the LC/MS-based metabolomics approach to assess metabolism

more in detail. An untargeted metabolomics approach was applied to the embryonic kidney mesenchyme cell line (mK4) treated with the MEK inhibitor UO126 to mimic genetic MAPK/ERK-deficiency *in vitro*. The LC/MS data of the non-treated cells, DMSO-treated cells, and the MEK-inhibited cells were analyzed by the partial least square's discriminant analysis (PLS-DA), one of the multivariate statistical analysis techniques. As a result, each group showed clear discrimination in both positive and negative detection mode while clustering well within their treatment group (Figure 2). Comparison of the MS2 spectrum patterns with online MS database revealed total of 38 significant different metabolites which are summarized in Table 1.

Of the significantly changed metabolites, only four, acetylasparagine, methylglutamic acid, xanthine, and oxidized glutathione, were up-regulated, while most differentially present metabolites were down-regulated. In particular, many of diminished metabolites identified by our LC/MS assay and differentially expressed transcripts (Kurtzeborn et al, manuscript in revision) were related to amino acid metabolism.

We next performed targeted metabolomics analysis aiming at identification of metabolic intermediates from glycolysis and mitochondrial metabolism, and quantification of principally altered metabolites. This revealed eight statistically different intermediate metabolites upon MAPK/ERK-deficiency: glucose, glucose-6-phosphate, 3-phosphoglyceric acid, phosphoenolpyruvate, ribose-5-Phosphate, citrate, ATP, and ADP, all of which are down-regulated by MAPK/ERK deficiency (Table 1). This quantitative intermediate metabolite result is well in line with our RNAseq results (Kurtzeborn et al, manuscript in revision), which indicated down-regulation of mitochondrial functions.

Our untargeted and targeted metabolomics analysis identified all together 46 metabolites (38 from untargeted and 8 from targeted) which are summarized in Table 1. Metabolic set enrichment analysis (MSEA) of identified metabolites through MetaboAnalyst revealed

glycolysis and gluconeogenesis, pentose phosphate pathway and starch and sucrose metabolism as the most altered metabolic pathways in the absence of MAPK/ERK activation (Figure 3A). Visualization of the actual metabolite level changes by heatmaps shows that most of the metabolic pathways, but particularly energy metabolism, were down-regulated upon MAPK/ERK-deficiency (Figure 3B). Table 2 summarizes MSEA analysis results by listing the contributing metabolites.

Integration of metabolomics and RNAseq results to the systems biology approach

Next, in order to conduct a more comprehensive analysis at the level of whole systems biology, we attempted an integrated analysis the information obtained from the metabolomics results and our recent RNAseq data. The basic idea of metabolic pathways is a kind of catabolism regulated by enzymes, where these metabolic pathways are composed of regulating enzymes and the metabolites as an end product. Here, we have obtained quantitative metabolite level changes in MAPK/ERK-deficient cells through a metabolomics approach, and gene expression level changes in MAPK/ERK-deficient nephron progenitors by RNAseq. The mutually meaningful relationship between metabolites and genes expression levels was investigated by integrating the two analysis results, and the results are summarized in Figure 4.

Among 46 identified metabolites, 18 metabolites were correlated to 25 differentially expressed genes (Figure 4) from our RNAseq data (Kurtzeborn et al, manuscript in revision). Most metabolite-gene interactions showed the same change patterns that presenting decreased measures for both. For example, we identified that the proline production-related enzymes PYCRL and PYCR2 were down-regulated, and their metabolite product, L-proline, was also diminished. As another example, we identified that the level of fatty acid synthase (FASN), which plays an important function in the production of palmitic acid, together with its end product palmitic acid are both significantly reduced. Conversely, in few cases, the correlation between the metabolite level and the gene level was opposite to each other. For instance,

subtypes of glutathione peroxidase family were down-regulated (GPX1, GPX3, GPX4, and GPX7), but the oxidized glutathione produced by these genes was increased demonstrating that transcriptional changes do not always translate into protein level differences. All the possible correlations between identified metabolites and DEGs are summarized in Table 3.

Integrated systems biology approach identified several metabolic pathways, which were affected by the MAPK/ERK-deficiency. One of these is glycine, which is the major regulatory metabolite with functions in antioxidant response and neuronal specification (34). We found that glycine and four glycine metabolism-related genes are down-regulated MAPK/ERK-deficient cells. These included serine hydroxymethyltransferase-2 (*Shmt2*), which is involved in the process of serine to glycine metabolism, sarcosine dehydrogenase (*Sardh*) involved in the process of sarcosine to glycine metabolism, glutathione synthetase (*Gss*) involved in glycine to glutathione metabolism, and glycine C-acetyltransferase (*Gcat*), which contributes to threonine to glycine processing. Another interesting metabolite identified here is proline, which also contributes to neuronal differentiation (28, 29). Proline metabolism is down-regulated in MAPK/ERK-deficient cells, and its direct regulators *Pycr2* (mitochondrial) and *Pycrl* (cytosolic) are also down-regulated in MAPK/ERK-deficient NPs. The correlations of metabolite-to-gene expression changes identified here are visualized in Figure 5.

Pyruvate effect on early stage kidney development

To investigate physiological consequences of identified metabolic changes we first assayed the effect of pyruvate on early kidney development. Embryonic day 11.5 (E11.5) kidneys were cultured for 72h *in vitro* as described earlier (35) under normal and different pyruvate concentration conditions. Cultured kidneys were immunostained with calbindin to visualize ureteric bud branching morphogenesis (Figure 6A). Without pyruvate kidney growth through branching morphogenesis was severely compromised (50-80% less tips) and the ratio of ureteric bud tip-to-trunk was obscure. Pyruvate supplementation with low doses,

concentrations less than 1.0 mM, improved the branching rate and pattern but were not completely rescued to the level seen with 1.0 mM pyruvate, which normally used in kidney culture medium. Interestingly, pyruvate concentration higher than 1mM resulted in different ureteric bud tip morphology and branching pattern as low concentrations (0-0.5mM) suggesting dosage-specific effects for this important metabolite.

Pycr1/2 dko mouse model shown decrease of Pax2 and Six2 levels in NPs

Our integrated metabolomics and transcriptomics data revealed that majority of the pathways involved in energy metabolism are down-regulated upon MAPK/ERK-deficiency. Down-regulation of proline metabolism is of particular interest as in addition to reduced metabolite itself, the expression of its regulatory genes *Pycr2* and *Pycrl*, which were recently shown to be essential for normal neuronal development (28, 29), were significantly diminished (Figure 6B).

To assess the physiological *in vivo* requirement of proline metabolism in kidney development, we utilized conventional inactivation of *Pycr1* and *-2* genes in mouse. We found that inactivation of single *Pycr* gene resulted in Mendelian ratios of homozygous *Pycr1*$^{-/-}$ and *Pycr2*$^{-/-}$ pups with grossly normal kidney morphology and histology. Similarly, the double knockout *Pycr1*$^{-/-}$*;Pycr2*$^{-/-}$ pups were born in Mendelian ratios and had grossly normal kidneys. Further characterization of *Pycr1*$^{-/-}$*;Pycr2*$^{-/-}$ mouse kidneys at postnatal day 1 (P1) revealed defects in NP population as detected by reduced number of PAX2-positive cells per ureteric bud and by premature differentiation of postnatal SIX2-positive NPs (Figure 6B). These results demonstrate that proline metabolism, which we identified here to depend on MAPK/ERK activation, is essential for the maintenance of NP population in developing kidney

DISCUSSION

Metabolomics is one of the emerging fields of 'omics' research to study global metabolic profiles in a variety of biological samples (36). Although metabolomics provides a functional

fingerprint of the physiology and pathophysiology, it requires complementation from the dynamic cellular and organismal functions. Thus, systems biology approach incorporates different 'omics' data that are required for functional linkages (37). Since metabolomics has potential as a linker between genotype and phenotype (38), it has been broadly and successfully used in systems biology studies (39) to gain a better understanding of complex biological systems (40-42). The metabolomics studies of mitochondrial dysfunction in kidney diseases are good example of the potential of metabolic approach (43, 44).

Congenital anomalies of the kidney and urinary tract (CAKUT) are common birth defects caused by abnormalities in kidney morphogenesis, which contribute to the growing worldwide chronic kidney disease burden (45-47). The spectrum of CAKUT phenotypes varies from mild renal hypoplasia with reduced nephron count, to hypodysplasia and to a complete lack of kidneys, condition known as agenesis or aplasia (48). The milder CAKUT forms such as reduced nephron mass due to hypoplasia are not life-threatening at early ages, but do possess increased risk of chronic kidney disease with cardiovascular co-morbidities later in life (1, 2). As the final nephron count in each individual is determined by renal morphogenesis during fetal development, any factors possibly affecting the rate and extend of nephrogenesis are of high interest.

There is increasing awareness of how mitochondrial dysfunction contributes to various acute and chronic pathologies. Kidney is one of the highly energetic organs that contains abundant mitochondria (49), and the malfunctioning mitochondria have significant effects on the pathogenesis of adult-onset kidney diseases (50). Therefore, mitochondria have emerged as promising therapeutic options for renal diseases (51, 52).

Detailed analysis of more than 5,000 DEGs observed in NPs from MAPK/ERK-deficient mice revealed (Kurtzeborn et al, in revision) that 30% of genes were related to mitochondrial energy metabolism including oxidative phosphorylation (18.87%) and mitochondrion (11.32%). In

particular, it was also confirmed that 40% of genes among the genes decreased by MAPK/ERK deficiency are related to mitochondrial metabolic activity including mitochondrial inner membrane (25.0%) and mitochondrion (15.0%). In addition, the reduction of energy metabolism-related metabolic pathways such as glycolysis, gluconeogenesis, and pentose phosphate pathway were identified here.

Through systems biology approach by integrating metabolomics and RNAseq data, we demonstrate that the MAPK/ERK activity of NPs significantly contributes to cellular metabolism, particularly for mitochondrial energy metabolism (Fig 3). In this study, we not only identified down-regulated genes and metabolites by MAPK/ERK deficiency, but also suggested the correlation between reduced metabolites and genes involved in their regulation through gene-metabolite integration analysis (Fig 4). Since the metabolic pathways are not fragmentary and is a complex process in which many genes and metabolites are interrelated, the overall metabolic flow map is presented by combining the results obtained in our experiments for a more effective understanding. As shown in metabolic pathway map in Fig 5, majority of genes and metabolites were down-regulated by MAPK/ERK deficiency, especially related with energy metabolism such as glycolysis, pentose phosphate pathway, glutaminolysis and as well as proline metabolism.

Some gene-metabolite correlations have shown the opposite direction, for example in which subtypes of the glutathione peroxidase family (GPXs) are up-regulated but their product oxidized glutathione (GSSG) levels are reduced. Although the expression of GPX genes that directly contribute to the production of GSSG was increased, it could be interpreted that the decrease in glutathione synthase (GSS) that produced glutathione by consuming glycine at a upper level eventually led to a decrease in overall GSSG expression. This total metabolomic approach can also be applied to decreased glutamine and glutamate and increased glutaminase (GLS) observed in glutaminolysis.

Production of pyruvate, one of the major metabolites playing an important role in mitochondrial metabolism, is strongly regulated by the glycolytic enzyme pyruvate kinase isozyme M2 (PKM2). Our results from kidney cultures in different pyruvate concentrations show dose-specific functions and suggest that low pyruvate availability may support collecting duct progenitor propagation, as ureteric buds were enlarged in 0-0.5mM concentrations, while high concentrations trigger differentiation. Importantly, MAPK/ERK signaling is a known pyruvate metabolism regulator through PKM2 (19), and PKM2 is expressed in the embryonic kidney (53). We also identified down-regulation of the proline production regulatory genes *Pycr2* and *Pycrl* and demonstrated reduced levels of proline metabolite in MAPK/ERK-deficient cells. This is very important result not only because the exact function of proline metabolism at organ or tissue level in developing kidney has remained unknown, but also due to its therapeutic potential as a metabolite that is easy to administrate.

MATERIALS AND METHODS

Gene Ontology and Pathway Analysis

To further analysis how MAPK/ERK-deficient nephron progenitor (NP) populations have different metabolic characteristics, we utilized our recent whole-genome RNAseq data (ref-our RNAseq paper). To interpret differentially expressed genes in NPs, we performed the pathway analysis using Cytoscape plug-in ClueGO to create a functionally organized gene ontology (GO). The GO_Cellular Component and KEGG ontology were used for GO analysis and we performed the GO analysis using total DEGs and up-regulated and down-regulated DEGs separately.

Metabolomics sample preparation

To investigate metabolic changes on NPs occurred by MEK inhibition, we analyzed metabolic changed of mK4 cell line derived from embryonic kidney mesenchyme through LC/MS based

metabolomics approach. Prior to cell harvest for metabolite extraction, mK4 cells were incubated with DMSO (0.1% v/v) or MEK inhibitor UO126 (15 μM) or without any treatment. After 24 hours incubation, cells were harvested using 0.25% Trypsin/EDTA treatment and washed with cold PBS. The metabolites were extracted by same method applied in our current RNAseq research (ref-our RNAseq paper). In brief, harvested cells were dissolved with 600 μl of methanol/chloroform solvent (2:1 v/v ratio), and two repeated steps of quick frozen with liquid nitrogen and thawing at room temperature were applied. Then, 200 μl of each of chloroform and distilled water were sequentially added, and metabolites were separated by following centrifugation at 15,000 g for 20 min at 4 °C. Finally, water soluble metabolites (upper phase after centrifugation) were dried using centrifugal vacuum evaporator. The middle phase (protein aggregate) after centrifugation were isolated and dissolved in 6M urea buffer and total protein concentration were measured to utilize on normalization.

Liquid chromatography-mass spectrometry (LC-MS) analysis

The ZIC-HILIC column (3.5 μm, 200 Å, 100 × 2.1 mm; Merck Millipore) and Acquity UPLC system (Waters, MA, USA) were used for liquid chromatography. The Q Exactive Focus Orbitrap Mass Spectrometer (Thermo Fisher Scientific) equipped with HESI sources were used for metabolites identification. All the detail parameters were exactly same as our our recent research (ref-our RNAseq paper), including liquid chromatographic separation and mass spectrometry experiment. In order to detect as many ions as possible, both positive and negative detection modes were used in LC/MS experiment. The inclusion list for PRM was shown as supplement materials (Table S2). The MS2 spectrum patterns comparison from the online MS database Metlin and high-resolution m/s from full MS experiment were applied to confirm target metabolites. All the measured data were normalized against total protein concentration which were measured using middle phase protein aggregate concentration.

Metabolmics analysis and systems biology approach

The multivariate statistical analysis was carried out using SIMCA-P version 11.0 program (Umetrics, Umeå, Sweden). To distinguish metabolic pattern differences from each experimental group, the supervised statistical method, partial least squares discriminant analysis (PLS-DA) analysis, was performed using the processed data from LC/MS positive and negative mode and statistically contributing metabolites on group separation on PLS-DA were identified. To further analyzing the identified metabolites, we performed Metabolite Set Enrichment Analysis (MSEA) thorough web-based analysis tool provided from MetaboAnalyst(Reference for Metaboanalyst), and the level of individual contributing metabolite on MSEA result were visualized by heatmap analysis in R package.

Pyruvate effect on embryonic kidney culture

E11.5 control mouse kidneys were cultured under different concentration of pyruvate supplementation for 72 hours. Cultured embryonic kidneys were analyzed via immunostaining using Six2 antibody to determine the effect of pyruvate concentration on ureteric bud branching.

Immunofluorescent staining and imaging

Postnatal kidneys at P1 of double knockout Pycr1/2 were collected and kidneys were fixed with 4% PFA, after which they were processed to paraffin embedding and sectioning according to standard procedures. Immunofluorescent staining and imaging procedures were performed as previously described (20). Primary antibodies used are CALBINDIN (Santa Cruz Biotechnology, sc-7691) PAX2 (Invitrogen, 71-6000) and SIX2 (ProteinTech, 11562-1-AP). Alexa Fluor-conjugated secondary antibodies (1:400; Jackson Immuno Research Laboratories) were used as secondary antibodies.

Author Contributions

H.N.K: Research design, experiment, analysis data, manuscript writing; K.K: Experiment, manuscript editing; X.J.: LC/MS experiment; S.P.: Manuscript editing; S.K.: Conceptualization of the research, manuscript writing and editing.

References

1. Bertram JF, Douglas-Denton RN, Diouf B, Hughson MD, & Hoy WE (2011) Human nephron number: implications for health and disease. *Pediatr. Nephrol.* 26(9):1529-1533.
2. Luyckx VA & Brenner BM (2010) The clinical importance of nephron mass. *J. Am. Soc. Nephrol.* 21(6):898-910.
3. Davidson AJ, Lewis P, Przepiorski A, & Sander V (2019) Turning mesoderm into kidney. *Semin. Cell Dev. Biol.*, (Elsevier), pp 86-93.
4. Kurtzeborn K, Kwon HN, & Kuure S (2019) MAPK/ERK Signaling in Regulation of Renal Differentiation. *Int. J. Mol. Sci.* 20(7):1779.
5. Costantini F & Kopan R (2010) Patterning a complex organ: branching morphogenesis and nephron segmentation in kidney development. *Dev. Cell* 18(5):698-712.
6. Oxburgh L (2018) Kidney Nephron Determination. *Annu Rev Cell Dev Biol* 34:427-450.
7. Hartman HA, Lai HL, & Patterson LT (2007) Cessation of renal morphogenesis in mice. *Dev Biol* 310(2):379-387.
8. Hinchliffe SA, Sargent PH, Howard CV, Chan YF, & van Velzen D (1991) Human intrauterine renal growth expressed in absolute number of glomeruli assessed by the disector method and Cavalieri principle. *Lab Invest* 64(6):777-784.
9. Ryan D*, et al.* (2018) Development of the Human Fetal Kidney from Mid to Late Gestation in Male and Female Infants. *EBioMedicine* 27:275-283.
10. O'Brien LL (2019) Nephron progenitor cell commitment: Striking the right balance. *Semin Cell Dev Biol* 91:94-103.
11. Li H, Hohenstein P, & Kuure S (2021) Embryonic Kidney Development, Stem Cells and the Origin of Wilms Tumor. *Genes (Basel)* 12(2).
12. Li H*, et al.* (2021) Postnatal prolongation of mammalian nephrogenesis by excess fetal GDNF. *Development* 148(10).
13. Brown AC, Muthukrishnan SD, & Oxburgh L (2015) A synthetic niche for nephron progenitor cells. *Dev. Cell* 34(2):229-241.
14. Volovelsky O*, et al.* (2018) Hamartin regulates cessation of mouse nephrogenesis independently of Mtor. *Proc Natl Acad Sci U S A* 115(23):5998-6003.
15. Liu J*, et al.* (2017) Regulation of Nephron Progenitor Cell Self-Renewal by Intermediary Metabolism. *J. Am. Soc. Nephrol.* 28(11):3323-3335.
16. Cargill K*, et al.* (2019) Von Hippel-Lindau Acts as a Metabolic Switch Controlling Nephron Progenitor Differentiation. *J Am Soc Nephrol* 30(7):1192-1205.
17. Conaghan J, Handyside AH, Winston RM, & Leese HJ (1993) Effects of pyruvate and glucose on the development of human preimplantation embryos in vitro. *J. Reprod. Fertil.* 99(1):87-95.
18. Butcher L, Coates A, Martin KL, Rutherford AJ, & Leese HJ (1998) Metabolism of pyruvate by the early human embryo. *Biol. Reprod.* 58(4):1054-1056.
19. Yang W*, et al.* (2012) ERK1/2-dependent phosphorylation and nuclear translocation of PKM2 promotes the Warburg effect. *Nat. Cell Biol.* 14(12):1295-1304.
20. Ihermann-Hella A*, et al.* (2018) Dynamic MAPK/ERK Activity Sustains Nephron Progenitors through Niche Regulation and Primes Precursors for Differentiation. *Stem Cell Reports* 11(4):912-928.

21. Kurtzeborn K, Kwon HN, & Kuure S (2019) MAPK/ERK Signaling in Regulation of Renal Differentiation. *Int J Mol Sci* 20(7).
22. Li Y*, et al.* (2015) p53 Enables metabolic fitness and self-renewal of nephron progenitor cells. *Development* 142(7):1228-1241.
23. Kimura T*, et al.* (2003) Impaired function of p53R2 in Rrm2b-null mice causes severe renal failure through attenuation of dNTP pools. *Nat Genet* 34(4):440-445.
24. Powell DR*, et al.* (2005) Rapid development of glomerular injury and renal failure in mice lacking p53R2. *Pediatr Nephrol* 20(3):432-440.
25. Kuo ML*, et al.* (2016) PYCR1 and PYCR2 Interact and Collaborate with RRM2B to Protect Cells from Overt Oxidative Stress. *Sci Rep* 6:18846.
26. Aguilera O*, et al.* (2016) Vitamin C uncouples the Warburg metabolic switch in KRAS mutant colon cancer. *Oncotarget* 7(30):47954-47965.
27. de Koning TJ (2017) Amino acid synthesis deficiencies. *J Inherit Metab Dis* 40(4):609-620.
28. Escande-Beillard N*, et al.* (2020) Loss of PYCR2 Causes Neurodegeneration by Increasing Cerebral Glycine Levels via SHMT2. *Neuron* 107(1):82-94 e86.
29. Stum MG*, et al.* (2021) Genetic analysis of Pycr1 and Pycr2 in mice. *Genetics* 218(1).
30. Bindea G*, et al.* (2009) ClueGO: a Cytoscape plug-in to decipher functionally grouped gene ontology and pathway annotation networks. *Bioinformatics* 25(8):1091-1093.
31. Shannon P*, et al.* (2003) Cytoscape: a software environment for integrated models of biomolecular interaction networks. *Genome Res.* 13(11):2498-2504.
32. Ashburner M*, et al.* (2000) Gene ontology: tool for the unification of biology. *Nat. Genet.* 25(1):25-29.
33. Kanehisa M & Goto S (2000) KEGG: kyoto encyclopedia of genes and genomes. *Nucleic Acids Res.* 28(1):27-30.
34. Avila A*, et al.* (2014) Glycine receptors control the generation of projection neurons in the developing cerebral cortex. *Cell Death Differ.* 21(11):1696-1708.
35. Ihermann-Hella A & Kuure S (2019) Mouse ex vivo kidney culture methods. *Kidney Organogenesis*, (Springer), pp 23-30.
36. Pang H, Jia W, & Hu Z (2019) Emerging applications of metabolomics in clinical pharmacology. *Clin. Pharmacol. Ther.* 106(3):544-556.
37. Kitano H (2002) Systems biology: a brief overview. *Science* 295(5560):1662-1664.
38. Fiehn O (2002) Metabolomics--the link between genotypes and phenotypes. *Plant Mol. Biol.* 48(1-2):155-171.
39. Weckwerth W (2003) Metabolomics in systems biology. *Annu. Rev. Plant Biol.* 54:669-689.
40. Nam H, Chung BC, Kim Y, Lee K, & Lee D (2009) Combining tissue transcriptomics and urine metabolomics for breast cancer biomarker identification. *Bioinformatics* 25(23):3151-3157.
41. McKillop AM & Flatt PR (2011) Emerging applications of metabolomic and genomic profiling in diabetic clinical medicine. *Diabetes Care* 34(12):2624-2630.
42. Atzler D, Schwedhelm E, & Zeller T (2013) Integrated genomics and metabolomics in nephrology. *Nephrology Dialysis Transplantation* 29(8):1467-1474.
43. Sharma K*, et al.* (2013) Metabolomics reveals signature of mitochondrial dysfunction in diabetic kidney disease. *J. Am. Soc. Nephrol.* 24(11):1901-1912.
44. Tran MT*, et al.* (2016) PGC1α drives NAD biosynthesis linking oxidative metabolism to renal protection. *Nature* 531(7595):528-532.
45. Luyckx VA, Tonelli M, & Stanifer JW (2018) The global burden of kidney disease and the sustainable development goals. *Bull. World Health Organ.* 96(6):414.
46. Jain S & Chen F (2019) Developmental pathology of congenital kidney and urinary tract anomalies. *Clin Kidney J* 12(3):382-399.
47. Anand S, Khanam MA, & Finkelstein FO (2014) Global perspective of kidney disease. *Nutrition in kidney disease*, (Springer), pp 11-23.

48. Murugapoopathy V & Gupta IR (2020) A Primer on Congenital Anomalies of the Kidneys and Urinary Tracts (CAKUT). *Clin. J. Am. Soc. Nephrol.* 15(5):723-731.
49. Bhargava P & Schnellmann RG (2017) Mitochondrial energetics in the kidney. *Nat Rev Nephrol* 13(10):629-646.
50. Emma F, Montini G, Parikh SM, & Salviati L (2016) Mitochondrial dysfunction in inherited renal disease and acute kidney injury. *Nat Rev Nephrol* 12(5):267-280.
51. Granata S, Dalla Gassa A, Tomei P, Lupo A, & Zaza G (2015) Mitochondria: a new therapeutic target in chronic kidney disease. *Nutr. Metab. (Lond.)* 12(1):49.
52. Szeto HH (2017) Pharmacologic Approaches to Improve Mitochondrial Function in AKI and CKD. *J. Am. Soc. Nephrol.* 28(10):2856-2865.
53. Gupta V & Bamezai RN (2010) Human pyruvate kinase M2: a multifunctional protein. *Protein Sci.* 19(11):2031-2044.

Table 1. Metabolite marker identification

Name	DMSO	UO126	Fold change (%)	p value	Detection mode
N-Acetylputrescine	517,92	86,02	-83,39	0,0452	Positive
L-beta-aspartyl-L-leucine (dipeptide)	2300,03	718,95	-68,74	0,0001	Positive
aspartylleucine	578,74	195,51	-66,22	0,0208	Negative
ATP	1181506,714	400539,4873	-66,10	0,006410875	Targeted
Glutamylleucine (dipeptide)	2401,49	832,05	-65,35	0,0002	Positive
ADP	15665432,16	5552987,351	-64,55	0,007259149	Targeted
Leucyl-Glutamate	904,59	327,07	-63,84	0,0442	Negative
Phosphoenolpyruvate	413249,6661	166906,85	-59,61	0,004737046	Targeted

Glutamylthreonine	137,95	56,98	-58,70	0,0208	Negative
5-Amino-6-(5'-phosphoribitylamino) uracil	2261,14	937,08	-58,56	0,0075	Negative
D-Ribose	529,23	237,75	-55,07	0,0442	Negative
Uracil	1104,46	530,84	-51,94	0,0442	Negative
Ribose-5-Phosphate	2967069,587	1471881,721	-50,39	0,026691008	Targeted
N-Acetylglutamine	964,50	541,66	-43,84	0,0367	Negative
Pyroglutamine	7049,93	3981,30	-43,53	0,0001	Positive
Dihydrothymine	214,58	124,68	-41,90	0,0442	Negative
Ribothymidine	1604,28	974,24	-39,27	0,0442	Negative
3-Phosphoglyceric acid	2212051,302	1387916,331	-37,26	0,032990339	Targeted
L-Aspartic acid	2187,44	1384,33	-36,71	0,0083	Positive
Palmitic acid	5091,69	3291,31	-35,36	0,0049	Negative
Asparaginylhistidine	410,91	269,75	-34,35	0,0485	Negative
5'-Methylthioadenosine	3815,56	2511,14	-34,19	0,0416	Positive
L-Tryptophan	2996,42	2001,86	-33,19	0,0026	Positive
Pyroglutamic acid	12625,70	8646,29	-31,52	0,0012	Positive

L-Leucine	49239,70	34975,68	-28,97	0,0083	Positive
Glycerophosphocholine	28559,80	20717,28	-27,46	0,0109	Positive
Citrate	6338539,807	4614380,619	-27,20	0,012019258	Targeted
Creatinine	65685,88	49458,70	-24,70	0,0001	Positive
Glucose	275261529,2	207639705,9	-24,57	0,011530427	Targeted
L-Threonine	8307,13	6406,17	-22,88	0,0002	Positive
L-Glutamine	29074,85	22457,10	-22,76	0,0009	Positive
Glucose-6-Phosphate	11482576,43	8901531,373	-22,48	0,024413224	Targeted
L-Glutamic acid	25101,95	20310,43	-19,09	0,0021	Positive
L-Phenylalanine	15609,50	12703,10	-18,62	0,0067	Positive
L-Acetylcarnitine	12948,78	10641,95	-17,82	0,0220	Positive
Creatine	64756,45	53431,98	-17,49	0,0039	Positive
Glycine	5983,78	5026,74	-15,99	0,0305	Positive
L-Tyrosine	16526,33	13884,15	-15,99	0,0020	Positive
L-Proline	34675,13	29584,80	-14,68	0,0050	Positive
Ornithine	5425,29	4683,48	-13,67	0,0345	Positive
L-Methionine	12073,33	10733,00	-11,10	0,0224	Positive

L-Carnitine	44474,68	39587,95	-10,99	0,0277	Positive
Oxidized glutathione	4685,70	6290,85	34,26	0,0005	Positive
Xanthine	361,89	546,31	50,96	0,0058	Negative
Methylglutamic acid	244,15	552,14	126,15	0,0266	Negative
Acetylasparagine	188,84	498,36	163,91	0,0049	Negative

Table 2. Metabolic set enrichment analysis (MSEA) of identified metabolites

	Tot. Cmpd	Hits	Statistic Q	Raw p	Holm p	FDR	Contributing metabolites
Glycolysis and Gluconeogenesis	25	3	89,015	2,31E-05	0,001521	0,000201	PEP, G6P, ADP
Pentose Phosphate Pathway	29	4	89,015	2,31E-05	0,001521	0,000201	D-ribose, R5P, G6P, ADP
Warburg Effect	58	7	73,823	0,000196	0,011377	0,001056	3PG, R5P, G6P, Citrate, ADP, Glutamate, Glutamine
Glycerolipid Metabolism	25	3	81,245	0,000721	0,041124	0,001413	3PG, ADP, Palmitic acid
Oxidation of Branched Chain Fatty Acids	26	3	85,332	0,001042	0,055225	0,001413	Acetylcarnitine, Carnitine, ADP
Valine, Leucine and Isoleucine Degradation	60	3	85,306	0,001043	0,055225	0,001413	Leucine, ADP, Glutamate
Bile Acid Biosynthesis	65	3	85,321	0,001046	0,055225	0,001413	Palmitic acid, ADP, Glycine
Alanine Metabolism	17	3	85,293	0,001049	0,055225	0,001413	Glutamate, ADP, Glycine

Amino Sugar Metabolism	33	3	85,251	0,001049	0,055225	0,001413	Glutamine, Glutamate, ADP
Pyrimidine Metabolism	59	4	85,276	0,001048	0,055225	0,001413	Glutamine, ADP, Uracil, Dihydrothymine
Glutathione Metabolism	21	5	85,291	0,001046	0,055225	0,001413	Pyroglutamic acid, ADP, Glutamate, Glycine, Oxidized Glutahione
Urea Cycle	29	5	85,242	0,001048	0,055225	0,001413	Glutamine, Glutamate, ADP, Ornithine, Aspartate
Ammonia Recycling	32	5	85,249	0,001049	0,055225	0,001413	Glutamine, Glutamate, ADP, Aspartate, Glycine
Arginine and Proline Metabolism	53	6	85,254	0,001047	0,055225	0,001413	Proline, Creatine, N-Acetyl putrescine
Glutamate Metabolism	49	6	85,255	0,001047	0,055225	0,001413	Aspartate, Glycine, ADP, Glutamine, Glutamate, Oxidized Glutathione
Purine Metabolism	74	7	81,184	0,000723	0,041124	0,001413	Glutamine, ADP, R5P, Xanthine
Glycine and Serine Metabolism	59	8	81,171	0,000723	0,041124	0,001413	3PG, ADP, Glycine, Methionine, Glutamate, Threonine, ADP, Ornithinine
Methionine Metabolism	43	3	50,595	0,005857	0,094401	0,007455	Glycine, Methionine, 5-Methylthioadenosine

Table 3. All the possible correlations between identified metabolites and differentially expressed genes

Metabolites				Genes				
	T-test	FC %	Up / Down	Gene Symbol	Name	padj	log2FC	Up / Down
5'-Methylthioadenosine (MTA)	0,0416	-34,19	down	SRM	spermidine synthase	2,00,E-05	-1,49	down
Acetylasparagine	0,0049	163,91	up	ASPA	aspartoacylase (Canavan disease)	5,22,E-04	3,50	up
				ACY3	aspartoacylase (aminocyclase) 3	1,41,E-02	-2,02	down
ADP	0,0073	-64,55	down	TAF9	TATA-box binding protein associated factor 9	6,17,E-03	2,17	up
				RRM2B	ribonucleotide reductase M2 B (TP53 inducible)	1,35,E-05	1,55	up
				CANT1	calcium activated nucleotidase 1	3,27,E-02	-1,07	down
				NME2	NME/NM23 nucleoside diphosphate kinase 2	3,81,E-06	-3,92	down
				NME4	NME/NM23 nucleoside diphosphate kinase 4	2,40,E-02	-1,14	down
				NME6	NME/NM23 nucleoside diphosphate kinase 6	2,53,E-06	-3,05	down
				TCIRG1	T cell, immune regulator 1, ATPase, H+ transporting, lysosomal V0 protein A3	1,15,E-03	-1,90	down
ATP	0,0064	-66,1	down	CANT1	calcium activated nucleotidase 1	3,27,E-02	-1,07	down
				NME2	NME/NM23 nucleoside diphosphate kinase 2	3,81,E-06	-3,92	down
				NME4	NME/NM23 nucleoside diphosphate kinase 4	2,40,E-02	-1,14	down
				NME6	NME/NM23 nucleoside diphosphate kinase 6	2,53,E-06	-3,05	down
				TCIRG1	T cell, immune regulator 1, ATPase, H+ transporting, lysosomal V0 protein A3	1,15,E-03	-1,90	down
				ADCY6	adenylate cyclase 6	2,68,E-06	-1,82	down
				POLR1A	polymerase (RNA) I polypeptide A	1,28,E-06	-1,18	down
				POLR1B	polymerase (RNA) I polypeptide B	1,75,E-02	-1,00	down
				POLR1C	polymerase (RNA) I polypeptide C	1,08,E-06	-2,01	down
				POLR1E	polymerase (RNA) I polypeptide E	1,05,E-03	-1,57	down
				POLR2E	polymerase (RNA) II (DNA directed) polypeptide E	2,63,E-06	-1,91	down
				POLR2F	polymerase (RNA) II (DNA directed) polypeptide F	7,20,E-04	-2,45	down
				POLR2I	polymerase (RNA) II (DNA directed) polypeptide I	3,39,E-08	-3,03	down
				POLR2J	polymerase (RNA) II (DNA directed) polypeptide J	1,19,E-03	-1,62	down
				POLR3C	polymerase (RNA) III (DNA directed) polypeptide C	5,90,E-04	-1,27	down
				POLR3D	polymerase (RNA) III (DNA directed) polypeptide D	5,22,E-04	-1,30	down
				POLRMT	polymerase (RNA) mitochondrial (DNA directed)	2,26,E-04	-1,94	down
Citrate	0,012	-27,2	down	ACO1	aconitase 1	2,74,E-05	-1,16	down
				CLYBL	citrate lyase beta like	3,70,E-02	-1,67	down
Creatine	0,0039	-17,49	down	CKB	creatine kinase	1,28,E-07	-2,52	down
Glucose	0,0115	-24,57	down	Hk1	hexokinase 1	1,52,E-02	-1,07	down
				GAA	glucosidase, alpha, acid	2,30,E-02	-1,34	down
				GANAB	alpha glucosidase 2 alpha neutral subunit	2,57,E-05	-1,08	down
Glucose-6-phosphate (G6P)	0,0244	-22,48	down	Hk1	hexokinase 1	1,52,E-02	-1,07	down
3-Phosphoglycerate (3PG)	0,033	-37,26	down	ACYP1	acylphosphatase 1	1,95,E-06	2,79	up
				ACYP2	acylphosphatase 2	4,88,E-02	1,99	up
				PGK1	phosphoglycerate kinase 1	1,67,E-06	-1,14	down
				PHGDH	3-phosphoglycerate dehydrogenase	6,80,E-16	-2,87	down
				PGAM1	phosphoglycerate mutase 1	1,14,E-08	-2,62	down
Glycerophosphocholine	0,0109	-27,46	down	Lypla1	lysophospholipase I	1,58,E-22	2,08	up
				Lypla2	lysophospholipase 2	1,61,E-09	-3,23	down
Glycine	0,0305	-15,99	down	SHMT2	serine hydroxymethyltransferase 2	8,62,E-09	-2,49	down
				SARDH	sarcosine dehydrogenase	6,67,E-06	-2,87	
				GSS	glutathione synthetase	5,44,E-03	-2,34	
				GCAT	glycine C-acetyltransferase	5,93,E-07	-2,82	
				GATM	glycine amidinotransferase	1,54,E-03	1,86	up
				GLDC	glycine decarboxylase	8,89,E-04	-1,36	down
				RARS	arginyl-tRNA synthetase	1,44,E-06	-1,08	down
				AMT	aminomethyltransferase	1,28,E-03	-1,89	down
L-Aspartic acid	0,0083	-36,71	down	ASPA	aspartoacylase (Canavan disease)	5,22,E-04	3,50	up
				ADSL	adenylosuccinate lyase	3,90,E-09	-1,7	down
				ACY3	aspartoacylase (aminocyclase) 3	1,41,E-02	-2,02	down
				CAD	carbamoyl-phosphate synthetase 2	2,00,E-11	-2,04	down
				AGA	aspartylglucosaminidase	3,94,E-02	1,13	up
				GOT2	glutamatic-oxaloacetic transaminase 2	2,60,E-08	-1,52	down
				ASNS	asparagine synthetase	1,35,E-02	-1,04	down
L-Carnitine	0,0277	-10,99	down	CPT1C	carnitine palmitoyltransferase 1c	4,75,E-02	-1,53	down
				CPT2	carnitine palmitoyltransferase 2	1,52,E-02	-1,16	down
L-Glutamic acid	0,0021	-19,09	down	GLS	glutaminase	3,15,E-22	2,08	up
				GOT2	glutamatic-oxaloacetic transaminase 2	2,60,E-08	-1,52	down
				GCLC	glutamate-cysteine ligase	9,20,E-10	1,49	up
				GCLM	glutamate-cysteine ligase	5,38,E-05	1,38	up
				ALDH18A1	aldehyde dehydrogenase 18 family, member A1	4,53,E-03	-1,12	down
				ALDH4A1	aldehyde dehydrogenase 4 family, member	1,53,E-02	-1,29	down

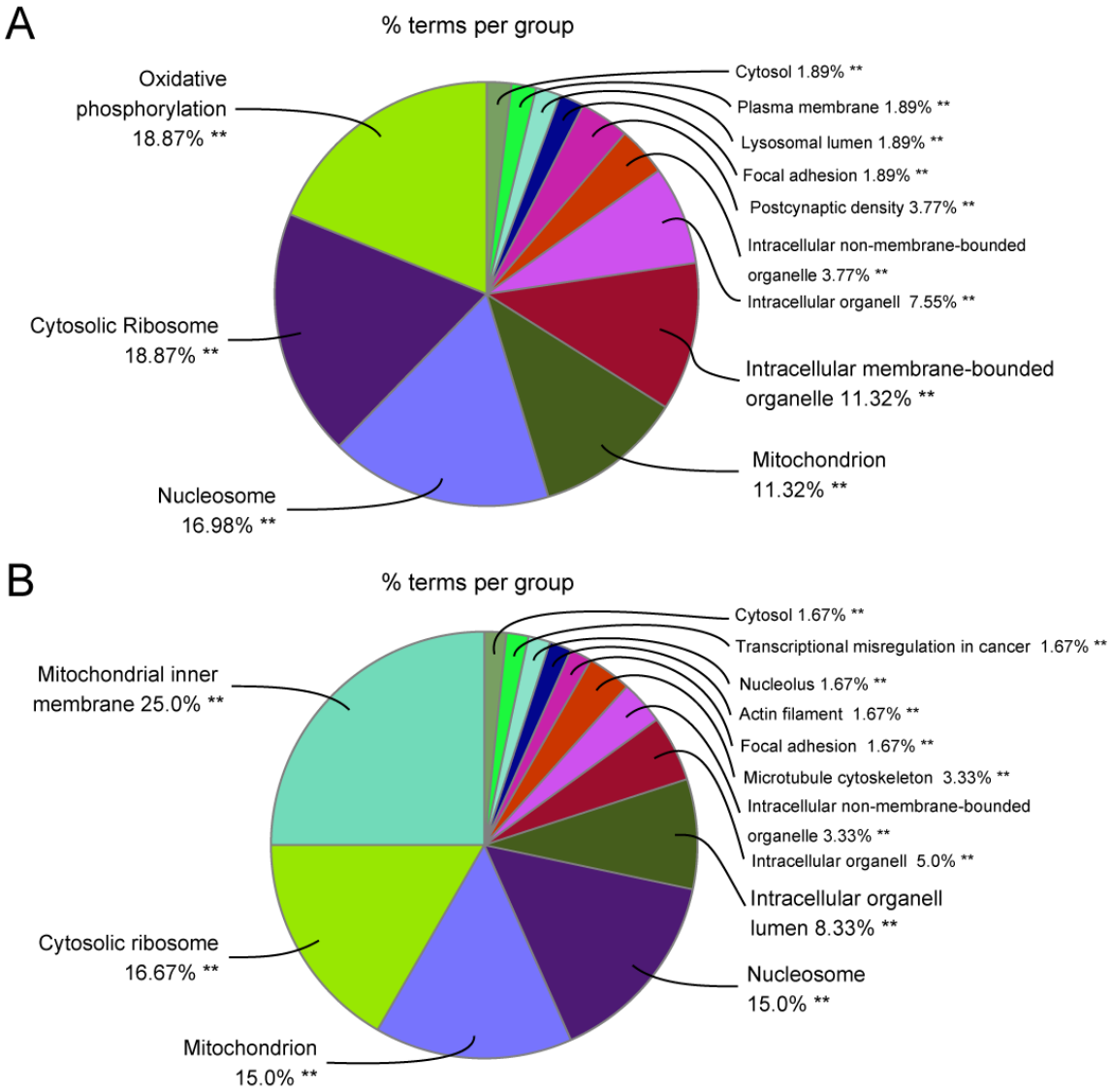

Figure 1. ClueGO analysis of differentially expressed genes in NPs

Overview pie chart with cellular component and KEGG pathway of the (A) total and (B) down-regulated differentially expressed genes (DEGs) in NPs. The percentage of genes per term is shown in each group. GO analysis was performed by Cytoscape plug-in application ClueGO. The pie chart shows the enriched signaling pathway categories based on the kappa coefficient of 0.5.

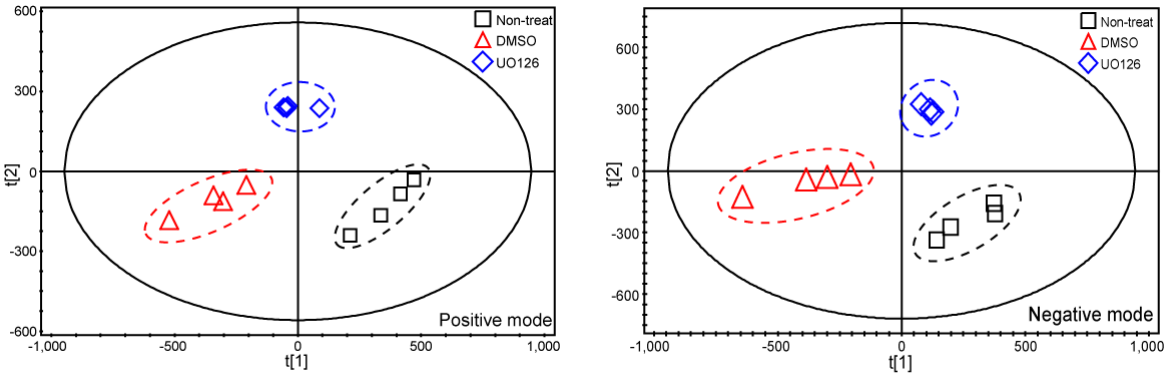

Figure 2. Partial least squares discriminant analysis (PLS-DA) analysis on positive and negative mode MS result on mK4 cell

PLS-DA score plot for m/z values of positive ($R^2X = 0.92$; $R^2Y = 0.991$; $Q^2Y = 0.968$; n = 1 + 4 components) and negative ($R^2X = 0.817$; $R^2Y = 0.999$; $Q^2Y = 0.992$; n = 1 + 1 components) detection mode of MS data. Each symbol represents the metabolic profile of an individual sample on each group (n=4). Black box indicates the non-treated group, red triangle indicates the DMSO treated group, and blue rhombus indicates the MEK inhibitor UO126 treated group.

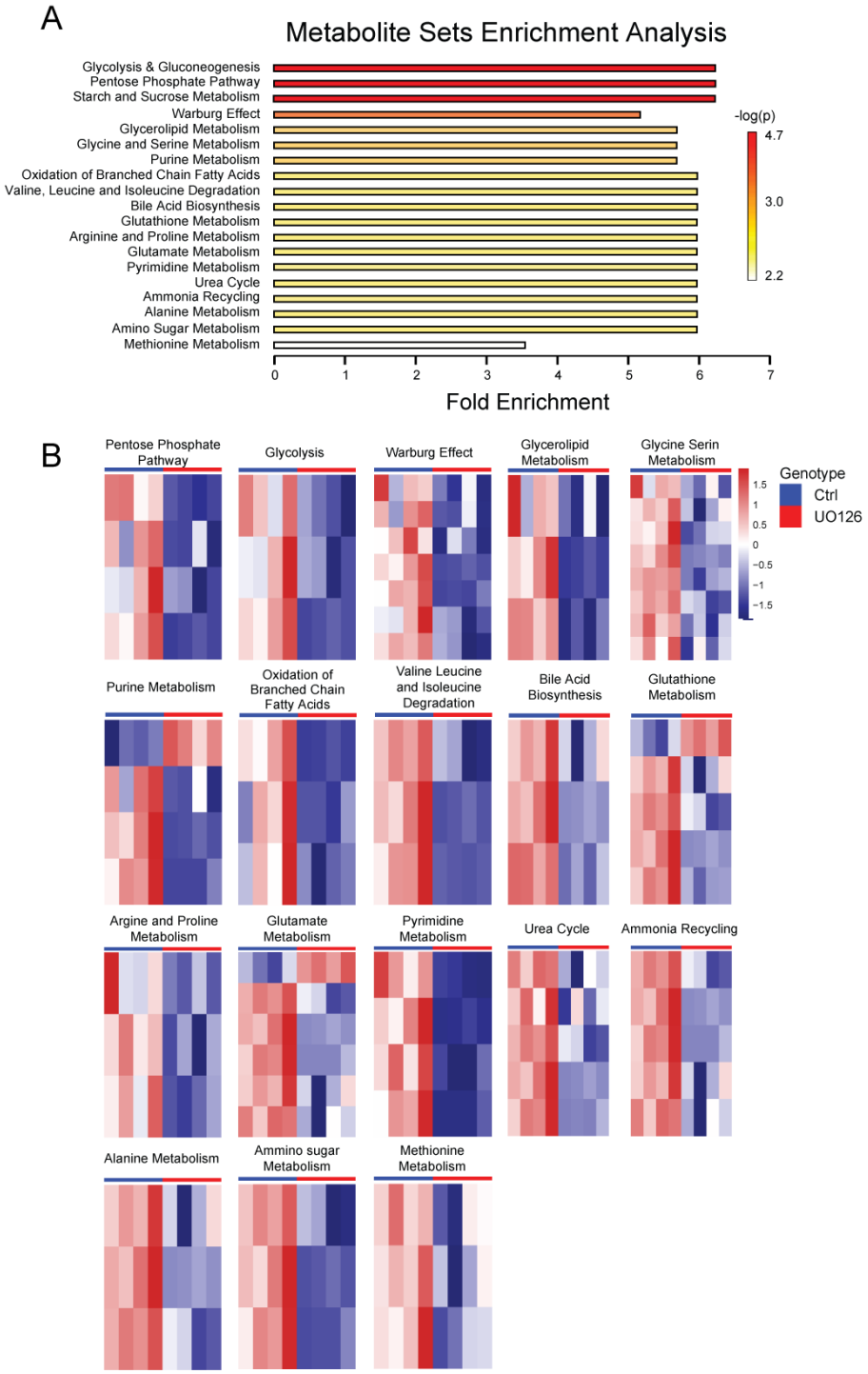

Figure 3. Metabolic Set Enrichment Analysis (MSEA) and the heatmap analysis.

A. Total 46 of identified metabolites are applied to MSEA to show the most altered metabolic pathways. The horizontal bar plot are ranked by adjusted p value by Holm-Bonferroni test. The color gradient is an indicator of how strongly a metabolic pathway changes, with the strongest changes pointing toward red and lower changes toward white. B. The heatmap analysis on the MSEA result to visualize the contributing metabolite level changes.

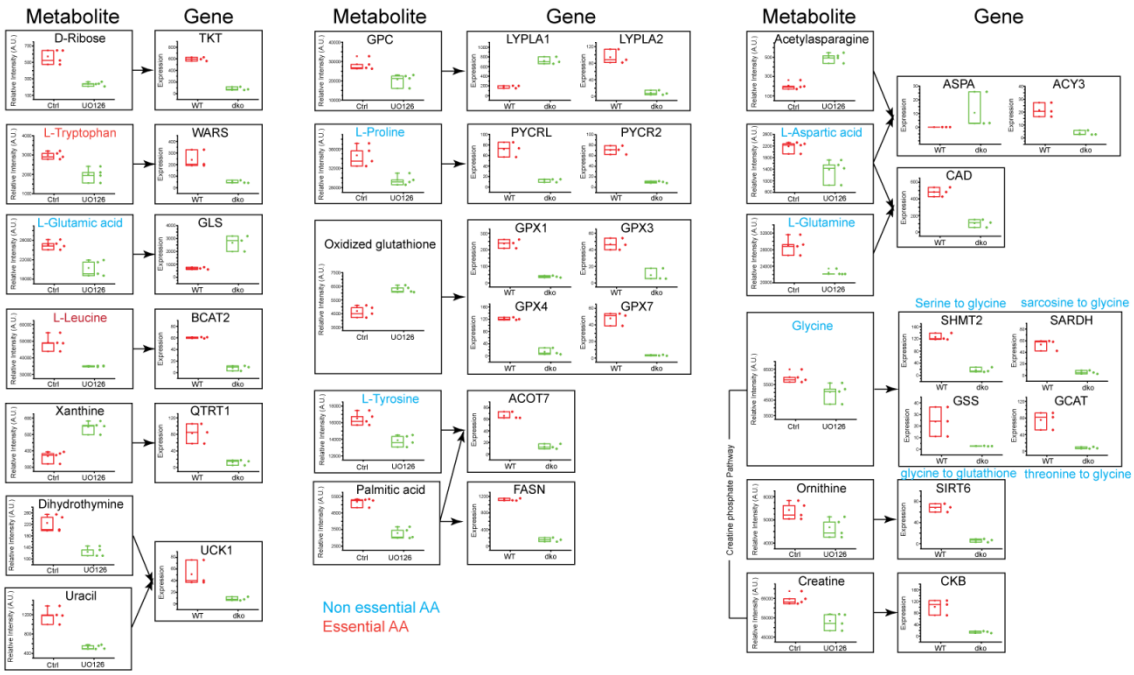

Figure 4. Cross linking metabolites and genes which are significantly changed in our RNAseq data.t

Quantitative metabolites and gene levels from metabolomics and RNAseq analysis were used to connect metabolite-gene correlation. Metabolites levels are measured from total 4 samples of DMSO and UO126 treated mK4 cell samples. Gene level changes are obtained from our recent RNAseq result (Kurtzeborn et al, in revision).

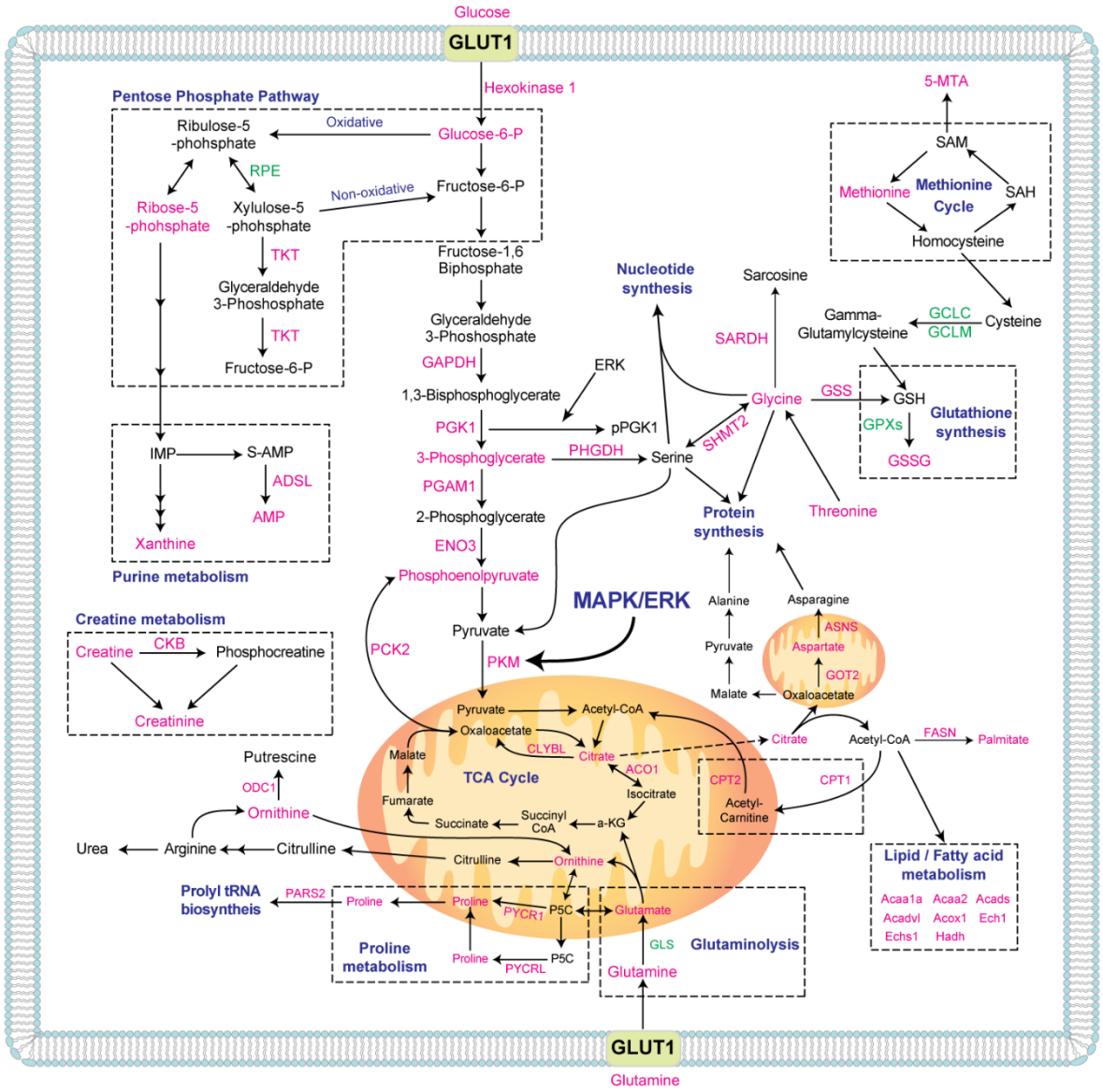

Figure 5. Overall metabolic pathway map by integrating metabolomics and RNAseq data.

Actual quantitated metabolites and enzymes are represented with magenta (down-regulated) and green (up-regulated). Dotted boxes represent metabolic pathways including metabolites and genes. RPE; Ribulose-phosphate 3-epimerase, TKT; Transketolase, GAPDH; Glyceraldehyde-3-phosphate dehydrogenase, PGK1; Phosphoglycerate kinase 1, PHGDH; D-3-phosphoglycerate dehydrogenase, PGAM1; Phosphoglycerate mutase 1, ENO3; Beta-enolase, PCK2; Phosphoenolpyruvate carboxykinase [GTP], PKM; Pyruvate kinase, ADSL; Adenylosuccinate lyase, CKB; Creatine kinase B-type, ODC1; Ornithine decarboxylase, PARS2; Probable proline--tRNA ligase, PYCR1; pyrroline-5-carboxylate reductase 1, PYCRL; Pyrroline-5-carboxylate reductase, GLS; Glutaminase, CLYBL; Citramalyl-CoA lyase, ACO1; Aconitate hydratase 1, CPT1; Carnitine palmitoyltransferase 1, CPT2; Carnitine

palmitoyltransferase 2, FASN; Fatty Acid Synthase, GCLC; Glutamate--cysteine ligase catalytic subunit, GCLM; Glutamate--cysteine ligase regulatory subunit, SARDH; Sarcosine dehydrogenase, SHMT2; Serine hydroxymethyltransferase 2, GSS; Glutathione synthetase, GPx; Glutathione peroxidase, ASNS; Asparagine synthetase, GOT2; Aspartate aminotransferase. Magenta represents down-regulated, green represents up-regulated.

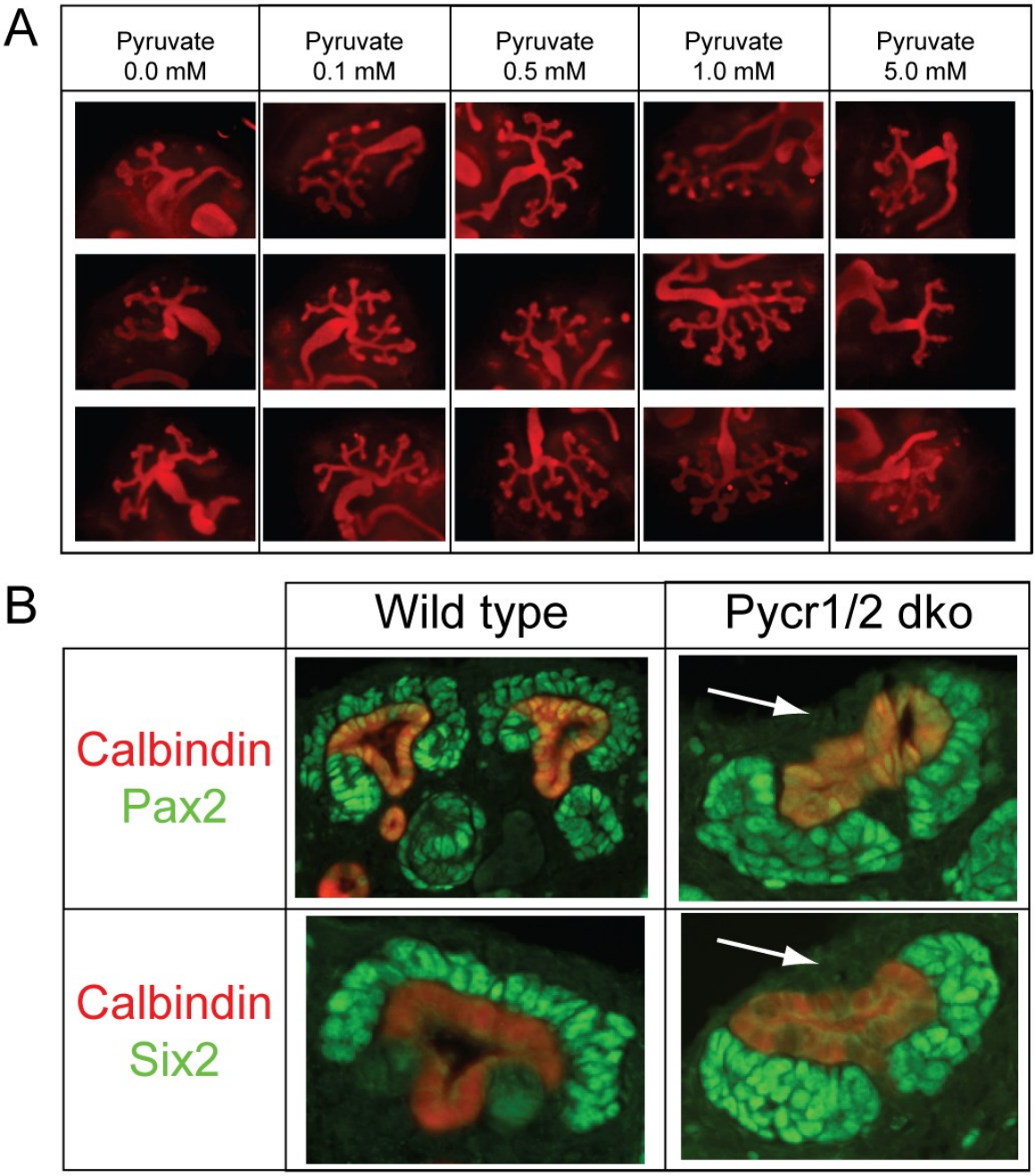

Figure 6. Pycr1/2 dko & pyruvate effect on kidney development

A. Embryonic kidneys at E11.5 were cultured for 72 hours under different concentration of pyruvate supplementation, and immunostained against Six2. B. Control (ctrl) and Pycr1/2 dko kidneys at P1 were immunostained for Pax2 and Six2 (nephron precursors) and Calbindin (ureteric bud [UB] epithelium). White arrow indicates the regions where Pax2 and Six2 signals are diminished.